REFINED ATCF MODEL FOR ABSORPTION LINE COLLISIONAL BROADENING AND SHIFT TAKING INTO ACCOUNT FINITE IMPACT PARAMETER AND EFFECT OF INTERNAL STATE UPON RELATIVE VELOCITY

V.V. Zuev and A.I. Petrova

Institute of Atmospheric Optics,
Siberian Branch of the Academy of Sciences of the USSR, Tomsk
Received August 5, 1990

Based on an analysis of elastic collisions and the use of the dependence of the absorption molecular velocity (v_1) and the impact parameter on the rotational quantum number J_1, the semiclassical ATCF model for line shifts and broadening in atmospheric gases has been refined.

The CO_2 molecule has been taken as a point of reference to compare the calculated line half-widths for self-broadened atmospheric CO_2 and the pressure-broadened N_2 and O_2 linewidths obtained by the refined ATCF model and the currently popular Robert-Bonamy CRB) model with the large quantity of experimental data presently available.

For small and especially large values of J_1, good quantitative agreement of our results with experiment has been found, which is achieved without any fitting conditions in contrast to the RB approach.

Within the framework of the proposed ATCF model, the line center shifts have been calculated taking into account certain factors which influence this parameter.

INTRODUCTION

The conventional approach to the description of the collisional broadening of spectral lines in molecular absorbers is based on the well-known Anderson-Tsao-Curnutte (ATC) model.[1,2] Frost[3] latter extended this theory to include the spectral line shift. The collision process in the ATCF theory is based on the following assumptions:

1) the absorption spectral line half-width is governed solely by the anisotropic part of the potential including electric, induction, and dispersion contributions, while the line center shift is governed by both the anisotropic and isotropic parts;

2) the molecules travel along straight trajectories with constant average velocity $\bar{v}$.

The above model provides a fairly good description of the spectral line broadening and shift parameters only for a limited range of values of the rotational quantum numbers (J_1) of the absorbing molecule in the transition $v_1J_1 \rightarrow v_fJ_f$. In so doing, consideration is generally given only to those molecular systems whose collisions are mostly characterized by multiple interactions alone. The ATCF model, however, fails to adequately describe the broadening parameters for transitions with large rotational quantum numbers (J_1). This justifies the search for other ways to describe the half-width (γ).

Among the novel approaches to the problem presently being considered most popular has been the BR-theory, which is based on the following assumptions:

1) the anisotropic potential includes not only the long-range part but also the short-range one;

2) for particles moving at a constant velocity $\bar{v}$, the minimum impact parameter appears to be smaller by a factor of < 1.5 than the gas-kinetic diameter (b_{gk}), whereas under anisotropic conditions they move along parabolic trajectories.

The authors of this approach4 claim that it is in agreement with the experimental data for various collisional partners both for the dependence of spectral line broadening on the rotational quantum number and on the temperature. In our opinion, however, the assumptions made in the work in question are not well-grounded. To begin with, the main contribution to the formation of the collision-induced spectral line shape comes from the long-range interactions with sufficiently large impact parameters rather than from the short-range interactions. In this case, straight trajectories appear to be more appropriate for describing the motion of the colliding particles, just as in the ATCF approach. Moreover, if we are to take into consideration the short-range part of the interaction potential, which is known to determine the repulsion of the particles, its influence cannot possibly lead to a decrease of the impact parameter due to parabolic curvature of the trajectory, as was assumed in the Bonamy-Robert model.

0235-6880/90/11 1019-15 $02.00

With the above remarks taken into account, the ATCF model proves more advantageous physically. However, it requires certain improvements. At least two essential points have been disregarded:

1) molecular collisions with impact parameters smaller than the gas-kinetic diameter (elastic collisions);

2) the dependence of the molecular velocity as well as of the impact parameter on the internal state of the absorbing molecule.

The first is related to the fact that for collisions of hard spheres the impact parameter cannot be smaller than the sum of the radii of the colliding molecules. Hence, the lower limit of integration over the impact parameter cannot be smaller than the gas-kinetic diameter, although in the classical ATCF approach this limit equals zero.

The second point follows from the fact that the interacting system must follow a Maxwell-Boltzmann velocity distribution related to the distribution of molecular energy states. The relative velocity v is then to depend upon the energy states of the absorption molecule (J_1).

The present paper describes a refined ATCF model which takes account of the above points and incorporates a procedure for determining the relative velocities and impact parameters associated with the energy states of the absorbing molecule. Also presented is a comparative analysis of the CO_2 absorption line shift and broadening obtained by the proposed model and those based on other approaches and experimental measurements.

1. PECULIARITY AND BACKGROUND OF OUR MODEL

1.1. REDETERMINATION OF THE INTEGRATION LIMIT OVER THE IMPACT PARAMETER IN THE ATCF MODEL AND ACCOUNT OF CONTRIBUTIONS OF HIGHER-ORDER INTERACTIONS TO THE SPECTRAL LINE SHIFT

It should be recalled that for the Lorentzian line shape ($i \to f$)

$$I_{if}(\omega) \sim \gamma_{if} \Big/ \left[(\omega - \omega_{fi} - \delta_{if})^2 + \gamma_{if}^2 \right] \qquad (1)$$

the half-width and shift parameters in the ATCF theory depend on the matrix elements of the scattering operator T

$$\gamma_{if} - i\delta_{if} = \frac{N}{2\pi c} \sum_g \rho_g \int dv \left[1 - T_{ii} T_{ff}^{+} \right]. \qquad (2)$$

Here $\int dv$ is the averaging operator over the impact parameter (b) and the relative velocities of interacting particles (v); g stands for the set of quantum numbers v_2 and J_2, and ρ is the density matrix.

The series expansion of the product of the matrix elements for the initial state T_{ii} and the final state T_{ff}^{*} (Eq. (2)) by the successive approx i mat ion technique under the initial condition $T(-\infty) = 1$ agrees with the exponential representation[6,7] for the second-order interaction[2]

$$T_{ii} T_{ff}^{+} \simeq \exp\left[-i\tilde{S}_2 - i\tilde{S}_1 - S_2 \right] \simeq 1 - i\tilde{S}_2 - i\tilde{S}_1 - S_2 \qquad (3)$$

The real part of the differential cross section

$$S_2 = \frac{1}{2} \left[\sum_{m_1 m_2} \frac{(J_1 m_1 J_2 m_2 | P^2 | J_1 m_1 J_2 m_2)}{(2J_2 + 1)(2J_1 + 1)} + \right.$$

$$+ \sum_{m_f m_2} \frac{(J_f m_f J_2 m_2 | P^2 | J_f m_f J_2 m_2)}{(2J_2 + 1)(2J_f + 1)} -$$

$$\left. - \sum_{\substack{m_1 m_1' \\ m_f m_f' \\ m_2 m_2' \\ M J_2'}} \frac{(J_1 l m_f M | J_1 m_1)(J_f l m_f' M | J_1 m_1')}{(2J_2 + 1)(2J_1 + 1)} \times \right.$$

$$\times (J_f m_f J_2 m_2 | P | J_f m_f J_2' m_2') \times (J_1 m_1' J_2' m_2' | P | J_1 m_1 J_2 m_2) \qquad (4)$$

as well as the imaginary parts of

$$\tilde{S}_1 = \sum_{m_1 m_2} \frac{(J_1 m_1 J_2 m_2 | P | J_1 m_1 J_2 m_2)}{(2J_2 + 1)(2J_1 + 1)} -$$

$$- \sum_{m_f m_2} \frac{(J_f m_f J_2 m_2 | P | J_f m_f J_2 m_2)}{(2J_2 + 1)(2J_f + 1)} \qquad (5)$$

and

$$\tilde{S}_2 = \frac{1}{2} \left[\sum_{m_1 m_2} \frac{(J_1 m_1 J_2 m_2 | P^2 | J_1 m_1 J_2 m_2)}{(2J_2 + 1)(2J_1 + 1)} - \right.$$

$$\left. - \sum_{m_f m_2} \frac{(J_f m_f J_2 m_2 | P^2 | J_f m_f J_2 m_2)}{(2J_2 + 1)(2J_f + 1)} \right] \qquad (6)$$

contain the matrix elements

$$(m | P | n) = \frac{2\pi}{\hbar} \int_{-\infty}^{\infty} \exp(i\omega_{mn} t)(m) H_c | n) dt, \qquad (7)$$

which depend on the interaction operator H_c, where $(J_f l m_f M | J_1 m_1)$ and $(J_f l m_f' M | J_2 m_2')$ are the Clebsh-Gordon coefficients, $J_i m_i$ and $J_f m_f$ are the quantum numbers of the initial and final states of the molecular absorber, $J_2 m_2 J_2' m_2'$ are the quantum numbers of the bath molecule. The latter interacts with the absorbing molecule.

According to the ATCF approach a transition to the relative velocity $\bar{v}$ is realized by substituting the relative velocity distribution function v

$$\int dv = \int_0^\infty dv \cdot vG(v) \int_0^\infty db 2\pi b = \bar{v} \int_0^\infty db 2\pi b$$

into the averaging operator

$$G(v) = \frac{4v^2}{\sqrt{\pi}\, v_b^3} \exp\left(-v/v_b\right)^2 \quad \text{with } v_b = \sqrt{\frac{\pi}{4}}\, \bar{v},$$

The expression for the rotational transition $i \to f$ ($J_i \to J_f$) or, if we replace J_i by $v_i J_i$ and J_f by $v_f J_f$, for the rovibrational transition can then be represented in the form

$$\gamma_{if} = \frac{N\bar{v}}{2\pi c} \int_0^\infty db 2\pi b S_2(b, f_n) \tag{8}$$

where f_n is the nonadiabaticity function.

To eliminate the divergence at the lower limit of the integral over b, we assume[1,2] that for any small impact parameter $b \le b_{og}$ strong collisions take place where the real differential cross section is given by

$$S_2(b, f_n) = 1. \tag{9}$$

Then the half-width

$$\gamma_{if} = \frac{N\bar{v}}{2c} \sum_g \rho_g b_{og}^2 \left[1 + S_2(b_{og}, f_n)\right] \tag{10}$$

depends on t types of intermolecular interactions through the real part of the cross section

$$S_2(b_{og}, F_n) = \int_{b_{og}}^\infty db\, b S_2(b_{og}, f_n) = \sum_t S_{2t}(b_{og}, F_n).$$

Since for the hard sphere collisions there are no impact parameters $b < b_{gk}$ the expression in square brackets in Eq. (4), must be replaced by

$$\left[\left\{1 - \left(b_{gk}/b_{og}\right)^2\right\} + S_2(b_{og}, F_n)\right]. \tag{11}$$

If the above factor is ignored, the values obtained using Eq. (10) will be overestimated by the value

$$\Delta\gamma = \frac{N\bar{v}}{2c} \sum_g \rho_g b_{gk}^2 ,$$

shown by the shaded part of the cross section (Fig. 1).

In practice, the overestimation, by $\Delta\gamma$ can be avoided by decreasing the multipole moments or by reducing the number of terms in the sum over the states of the molecule broadening. Unfortunately, this provides a consistent description of the γ-parameter only for the spectral region where the experimental data have been fit to the calculated values of γ. A special fitting is required for other spectral regions.

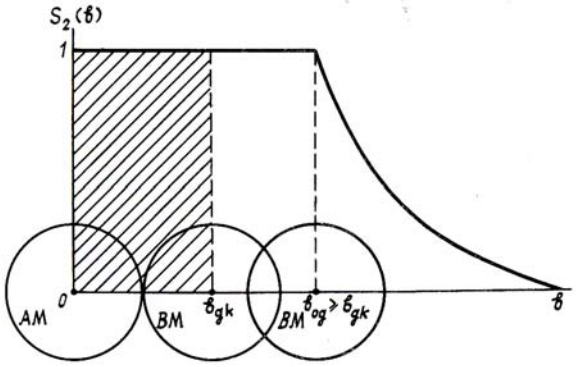

FIG. 1. Closest possible approach distances between the absorption molecule (AM) and the bath molecule (BM).

Unlike the ATC approach, our refined model describes the γ-parameters well for any set of quantum numbers J_1 and any collisional partners that do not affect the values of the multipole moments.

Let us proceed now to a derivation of the line center shifts. To this end, we expand the real and imaginary parts of the exponent in Eq. (3) in a series separably to give the integrand

$$\mathrm{Im}\left(1 - T_{ii} T_{ff}^*\right) \cong \left(\tilde{S}_2 + \tilde{S}_1\right)\left(1 - S_2\right), \tag{12}$$

which allows for the contributions of higher-order interactions (up to fourth order).

As is well known, the expression for δ_{if} in the ATCF approach is written as[3]

$$\delta_{if} = -\frac{N\bar{v}}{c} \sum_g \rho_g \int_0^\infty db\, b\left[\tilde{S}_2(b, f_n) + \tilde{S}_1(b, f_n)\right] \tag{13}$$

Unlike Eq. (13), the expression for the line shift obtained with the help of Eq. (12) is described by an additional contribution from the integrand $[1 - S_2(b, f_n)]$ (Ref. 8):

$$\delta_{if} = -\frac{N\bar{v}}{c} \sum_g \rho_g \int_0^\infty db\, b\left[\tilde{S}_2(b, f_n) + \tilde{S}_1(b, f_n)\right] \times$$

$$\times \left[1 - S_2(b, f_n)\right]. \tag{14}$$

In Eq. (14) according to the relation

$$\left[\tilde{S}_2(b, \tilde{f}_n) + \tilde{S}_1(b, \tilde{f}_n)\right]\left[1 - S_2(b, f_n)\right] = 0 \tag{15}$$

for $b \le b_{og}$, which follows from Eq. (9), the lower limit of integration over b is equal to b_{og}. The condition

$$S_2(b'_{og}, f_n) + \tilde{S}_2(b'_{og}, \tilde{f}_n) = 1 \qquad (16)$$

introduced in Refs. 3 and 8, gives the value b'_{og}, which is different from b_{og}, and, accordingly, a different lower limit (b'_{og}) of integration over b.

In our opinion, the problem of spectral broadening and line shift should be dealt with from one and the same standpoint, relying upon the same conditions and assumptions. Only such an approach can reveal all the limitations of the model. For instance, the above fitting manipulations used to calculate the γ-parameters will surely affect the values of δ, especially in the case of Eq. (14). This is because the experimental value of $\gamma_{ex} = \gamma'$ [expression (10), q_1, q_2] $= \gamma'$ [expression (10 – $\Delta\gamma$, q'_1, q'_2], for different calculational procedures will give values of quadrupole moments $q_1 \neq q'_1$ and $q_2 \neq q'_2$, whose contributions $\tilde{S}_2(q_1, q_2) \neq \tilde{S}_2(q'_1, q'_2)$ and $S_2(q_1, q_2 \neq S_2(q'_1, q'_2)$ which determine the line shift, can result in values of $\delta(q_1, q_2)$ and $\delta(q'_1, q'_2)$ which differ drastically from each other. On the other hand, conditions (16) and (9) yield the different values b_{og} and b'_{og} and, correspondingly, different γ and δ': ($\gamma(b_{og}) \neq \gamma(b'_{og})$ and $\delta(b_{og}) \neq \delta(b'_{og})$).

1.2. SELECTION PROCEDURE FOR THE ABSORBING PARTICLE VELOCITY

According to the Anderson theory (Fig. 2, scheme *a*) the average collision velocity is taken to be the average velocity of particle motion $\bar{v} = \sqrt{\bar{v}_1^2 + \bar{v}_2^2}$, equal to the rms average of the absorber $\bar{v}_1 = \sqrt{\frac{8kT}{\pi m}}$ and broadener $\bar{v}_2 = \sqrt{\frac{8kT}{\pi m}}$. In fact, however, the particles of the interacting system must obey the Maxwel1-Boltzmann velocity distribution, which, in turn, is related to the molecular energy state distribution. It should be recalled that for impact parameters $\geq 1.5 \cdot b_{gk}$ the particles move along straight lines.[7]

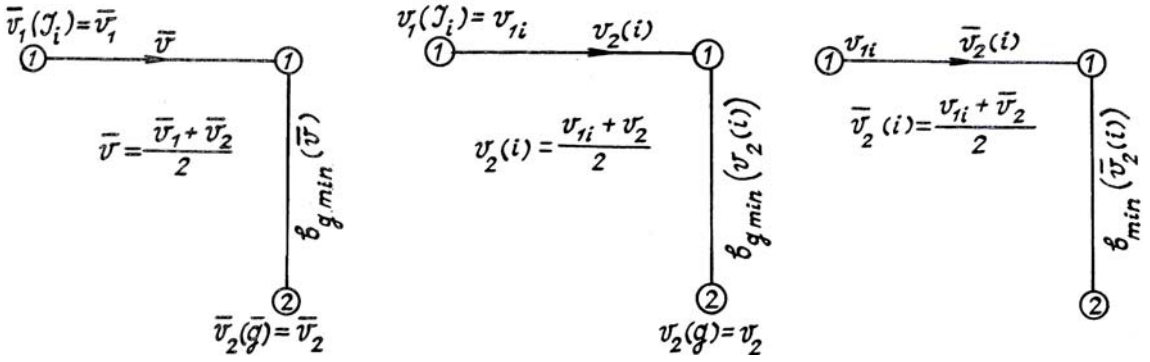

a *b* *c*

The Anderson theory *Our model*

FIG. 2. Modeling of the collision process: a) collision between the first and the second molecules travelling with average velocities $\bar{v}_1$ and $\bar{v}_2$, respectively, b) collision of two particles travelling with velocities $v_1(J_1)$, $v_2(g)$ depending on their states J_1 and g; c) same as in b upon averaging over the g-states of the bath molecule. The first and the second particles have the velocity $v_1(J_1)$ and $\bar{v}_2$, respectively.

Let the first colliding (absorbing) molecule move at the velocity $v_1(i)$ and be in a fixed energy state i, while the second (buffer) molecule have the velocity v_g and be in the state g (Fig. 2, diagram *b*). Averaging over the states of the second molecule gives the average velocity of the bath $\bar{v}_2$. The collision is then characterized by the average relative velocity

$$\bar{v}_2(i) = \sqrt{v_1^2(i) + \bar{v}_2^2} \qquad (16)$$

(Fig. 2, diagram *b*) depending on the internal state of the first molecule.

To obtain the minimum impact parameter $b_{min}(v_1(i), \bar{v}_2)$ (Fig. 2c), the truncation equation[1,2] is solved for $\bar{v}_2(i)$ and, upon averaging over the bath states, the resulting values $b_{q\min}(v_1(i), \bar{v}_2, q)$, become equal to $\bar{b}_{min}(i)$.

Our starting point is to find the values of parameters $\bar{b}_{min}$ and $\bar{v}_2$ for the most heavily populated rotational state of the first molecule J_{max}, whose most probable velocity is known:

$$v_1(J_{max}) = \sqrt{\frac{2kT}{m_1}}.$$

We then obtain $\bar{v}_2(J_{max})$ from Eq. (16), and the minimum impact parameter

$$\bar{b}_{\min}(J_{\max}) = \sum_g \rho_g b_{g\min}(J_{\max}) \qquad (17)$$

obtained by averaging over the bath states g depends on the values of $b_{g\min}(J_{\max})$ obtained in the traditional way Eq. (9). For the remaining states i, the values of $\bar{b}_{\min}$ and $\bar{v}_2$ are determined by the relation

$$\bar{v}_2(J_{\max})\cdot\bar{b}_{\min}(J_{\max}) = \bar{v}_2(i)\cdot\bar{b}_{\min}(i) = \text{const}, \qquad (18)$$

which represents the well-known law of conservation of momentum. It is assumed that

$$\bar{v}_2(J_{\max}) = \sqrt{v_1^2(J_{\max}) + \bar{v}_2^2}$$

The values of $\bar{b}_{\min}$ obtained using our model for different interacting partners are listed in Table I alongside the values of b_{gk} (Ref. 9) and b_{true} (Ref. 5) (b_{true} introduced in Ref. 5 is interpreted as the true minimum head-on impact parameter). The relevant values of the molecular parameters of the Interacting particles are given in Table II.

It can be seen from Table I that the so-called true minimum head-on impact parameter b_{true} in all of the cases is smaller than b_{gk}, which is not the case for the elastic interaction. Our values of $\bar{b}_{\min}(i)$ even for large J_1 are within the range of ~ $1.5b_{gk}$, characterized by straight trajectories of the relative motion of the interacting particles. Only in the molecular medium CO_2–O_2 for $J_1 > 60$ does $\bar{b}_{\min}(i)$ become $\leq 1.5b_{gk}$. In particular, $\bar{b}_{\min}(J_1 = 80) \approx 1.4b_{gk}$. Using the scheme of obtaining $\bar{v}_2(i)$ in terms of $v_1(i)$ via formula (16) we may show in the example of the molecular medium of CO_2–CO_2 that for $T = 300$ K the velocities of the absorbing molecules for small J_1 (e.g., $v_1(J_1) = 3.17 \cdot 10^4$ cm/s) and large J_1 (e.g., $v_1(J_1 = 50) = 4.23 \cdot 10^4$ cm/s) differ from the average molecular velocity ($\bar{v}_1 = 3.8 \cdot 10^4$ cm/s) by 10–15%. Such a variation in the velocity naturally will greatly affect the values of γ and δ obtained while calculating these relaxational parameters for small and large J_1.

TABLE I. Impact parameters (Å) for CO_2 as the absorbing molecule.

Mixture	b_{true} Ref. 5	b_{gk} Ref. 9	Our values	
			$\bar{b}_{\min}(J_1 = 0)$	$\bar{b}_{\min}(J_1 = 80)$
CO_2–CO_2	4.27	4.51	7.03	6.74
CO_2–N_2	3.88	4.12	6.9	6.1
CO_2–O_2	3.8	4.05	6.53	5.7

TABLE II. Molecular parameters of interacting particles.

Gas	g(DÅ)	E(10^{-12}erg)	B_0(cm^{-1})	α^*(Å^3)	$\alpha_\parallel$ (Å^3)	$\alpha_\perp$(Å^3)	$\alpha_\parallel - \alpha_\perp$(Å^3)
CO_2	6.0	22.06	0.39	2.65	2.97	1.3	1.6
N_2	3.6	24.85	2.0	1.75			0.93
O_2	3.0	20.03	1.438	1.6			1.14

• — polarizability for the vibrational ground state.

1.3. DERIVATION OF EXPRESSION FOR γ AND δ IN TERMS OF $\bar{b}_{\min}(i)$ AND $\bar{v}_2(i)$

In averaging over collisions between the bath molecules in the various g-states there is no necessity to average over the velocities of the relative motion during the collisions, for, as shown above, the velocity can be determined fairly well for particular states of the particles. Hence, for the rovibrational transition $v_iJ_i \to v_fJ_f$ (hereafter referred to as $i \to f$) in the expression for the half-width

$$\gamma_{1f} = \frac{N}{c}\sum_g \rho_g v'_g \int_{b_{gk}}^{\infty} db'_g b'_g S'_2 \qquad (19)$$

and the shift written in terms of the second

$$\delta_{1f} = -\frac{N}{c}\sum_g \rho_g v'_g \int_{b'_{g.min}}^{\infty} db'_g b'_g [\,\tilde{S}'_2 + \tilde{S}'_1\,] \qquad (20)$$

and the fourth-order interactions

$$\delta_{1f} = -\frac{N}{C}\sum_g \rho_g v'_g \int_{b'_{g.min}}^{\infty} db'_g b'_g \left[\tilde{S}'_2 + \tilde{S}'_1\right]\left[1 - S'_2\right] \tag{21}$$

All that remains is to integrate over the parameters b'_g. Later, for the sake convenience, we omit the subscript min used with the impact parameter. The prime in Eqs. (19), (20) and (21) means that, when considering the first element of the sum (S_{21}) of the cross section function S_2 describing the collision with an absorbing molecule in the i-state, the following substitutions are to be made: $v'_g \to v_g(i)$ and $b'_g \to b_g(i)$. To calculate the element $S_{2f} = S'_{2f}(v'_g, b'_g)$, use is made of the substitutions $v'_g = v_g(f)$ and $b'_g = b_g(f)$. Similar manipulation is applied to S_{2m}, which accounts for the correction between the energy levels i and f and is described by the parameters

$$v'_g = v_g(i, f) = \frac{v_g(i) + v_g(f)}{2},$$

$$b'_g = b_g(i, f) = \frac{b_g(i) + b_g(f)}{2}.$$

In the general case, in which all the collisions between the absorbing molecule and the bath particles are considered under the following conditions:

$$\begin{cases} S_{21}\left(b_g(i)\right) = \frac{1}{2}; \\ S_{2f}\left(b_g(f)\right) = \frac{1}{2}; \end{cases} \quad S_{2mid}\left(b_g(i,f)\right) = 0$$

in the derivation of $b_g(i)$ and $b_g(f)$, the half-width, after integrating over the impact parameter from b_{gk} to ∞, takes the form

$$\gamma_{1f} = \frac{N}{2c}\sum_g \rho_g \left[v_g(i)\, b_g^2(i) \times \right.$$

$$\times \left\{\eta(i) + S_{21}\left(b_g(i), v_g(i), F_n\right)\right\} + \left\{i \to f\right\} +$$

$$\left. + v_g(i,f)\, b_g^2(i,f)\, S_{2m}\left(b_g(i,f), v_g(i,f), F_n\right)\right] \tag{22}$$

where

$$\eta(i) = 1 - \left(b_{gk}/b_g(i)\right)^2/2. \tag{23}$$

Averaging over the energy structure $\sum_g \rho_g$ of the buffer molecules makes it possible to pass over to the average velocity $\bar{v}_2$ at fixed values of $v_1(i)$ and $v_1(f)$ of the absorbing particle as well as to the corresponding parameters $\bar{b}(i)$ and $\bar{b}(f)$. The latter approximation together with the mean value theorem[11] allow us to separate out that part of the collision cross section that depends on the impact parameter[10]

$$S_2^t(\bar{b}, \bar{v}, f_n) = \frac{\lambda\left(\bar{b}_{mid}, \bar{v}, f_n\right)}{\bar{b}^{ht}}, \tag{24}$$

and, with the help of using Eq. (9), after carrying out the integrations in Eqs. (19) and (21) we get the following expressions:

$$\gamma_{1f} = \frac{N}{2c}\sum_g \rho_g \left[\left\{ \bar{v}_2(i)\, \bar{b}^2(i)\left(\bar{\eta}(i) + \bar{S}_{21}\right)\right\} + \right.$$

$$\left. + \{i \to f\} + \bar{v}_2(i,f)\, \bar{b}^2(i,f)\, \bar{S}_{2m}\right], \tag{25}$$

$$\delta_{1f} = -\frac{N}{2c}\sum_g \rho_g \left[\left\{ \bar{v}_2(i)\, \bar{b}^2(i)\left(\tilde{\bar{S}}_{21} - \tilde{\bar{S}}_{11}\right)\right\} - \{i \to f\}\right] \tag{26}$$

with $\bar{\eta}(i)$ determined as in Eq. (23). The symbols $\bar{S}_2$ and $\tilde{\bar{S}}_{2(1)}$ correspond to the real and imaginary parts, allowing for the t type interaction

$$\bar{S}_{21} = \sum_t \frac{2}{(h_t - 2)} \frac{\lambda_{2t}\left(\bar{b}_{mid}(i), f_n\right)}{\bar{b}^{ht}(i)},$$

$$\tilde{\bar{S}}_{11} = \tilde{S}_{11}\left(\bar{b}(i), \bar{v}_2(i)\right)$$

The derivation of the expression for the line center shift (26) written in terms of $\bar{v}_2(i)$, $\bar{v}_2(f)$ and $\bar{b}(i)$, $\bar{b}(f)$ takes account of the first- and second-order interactions. For $\bar{v}_2(i, f)$ and $\bar{b}(i, f)$ the expression for the half-width is given by

$$\gamma_{1f} = \frac{N}{2c}\bar{v}_2(i,f)\, \bar{b}^2(i,f) \sum \rho_g \left[\bar{\eta}(i,f) + \bar{S}'_2\right], \tag{27}$$

where

$$\bar{\eta}(i, f) = 1 - \left(b_{gk} / \bar{b}(i, f)\right)^2;$$

$$\bar{S}'_2 = \bar{S}_{21} + \bar{S}_{2f} + \bar{S}_{2m};$$

$$\bar{S}_2 = \sum_t \frac{2}{(h_t - 2)} \frac{\lambda_{2t}\left(\bar{b}_{mid}(i,f), \bar{v}_2(i,f), f_n\right)}{\bar{b}^{ht}(i,f)}.$$

Making use of the same notation ($\bar{v}_2(i, f)$ and $\bar{b}(i, f)$), expression (21) for the line center shift, which allows for contributions in the interaction up to fourth-order, can be rewritten as

$$\delta_{if} = -\frac{N}{2c}\cdot\bar{v}_2(i,f)\,\bar{\delta}^2(i,f)\sum_g \rho_g \frac{\tilde{\lambda}_1\left(\bar{\delta}_{mid}(i,f),\ \bar{f}_n\right)}{\bar{\delta}^{hl}(i,f)}\times$$

$$\times\left[\frac{2}{(h_l-2)}-\sum_t\frac{2}{(h_l+h_t-2)}\frac{\lambda_{2t}\left(\bar{\delta}_{mid}(i,f),\ f_n\right)}{\bar{\delta}^{ht}(i,f)}\right]. \quad (28)$$

The values of l, t, h_i, and h_t versus the summands $\lambda_1(t)$ given by the above formulas are listed in Table III. The subscripts l and t indicate the type of interaction, where l and t refer to the imaginary and real parts of the cross section, respectively, and h_l and h_t are the power of the impact parameter.

TABLE III. The parameters h_l, h_t, $\tilde{\lambda}_l$, and λ_{2t} as functions of the summands (l, t).

l, t	1	2	3	4	5	6
h_l	5	5	4	6	6	8
$\tilde{\lambda}_l$	$\tilde{\lambda}^{**}_{1nnd}$	$\tilde{\lambda}_{1dis}$	$\tilde{\lambda}_{2pp}$	$\tilde{\lambda}_{2pq}$	$\tilde{\lambda}_{2qp}$	$\tilde{\lambda}_{2qq}$
h_t	4	6	6	8	10	
λ_{2t}	λ_{2pp}	λ_{2pq}	λ_{2qp}	λ_{2qq}	λ_{2dis}	

** — λ_{lind} characterizes the induction interaction.

2. CALCULATION OF CO_2 SPECTRAL LINE HALF-WIDTHS AND SHIFTS

Consider the relaxational characteristics (γ, δ) of the nonpolar molecular .media CO_2—N_2, O_2, and CO_2, whose corresponding impact parameters, as shown in Table I, are fairly large ($\sim 1.5 \cdot b_{gk}$).

2.1. CALCULATED HALF-WIDTHS

Figure 3 presents the ATC-calculated half-widths due to broadening $\left(\gamma_{CO_2\text{-}O_2}\right)$ for the electrooptic parameter $q_{CO_2} = 3.6$ and 4.3 DÅ most frequently reported in the literature (e.g., Refs. 5 and 16). Curves 1 describe only the quadrupole-quadrupo1e contribution, while curves 2 also take into account the dispersion contribution to the interaction of the colliding particles. It can be seen that the account of the dispersion contribution in the conventional ATC model leads to a sharp decrease in the half-width, and for $J > 30$ gives negative values of γ, which are meaningless from the physical standpoint. Therefore, a number of authors[5,18,17] have tried to avoid these difficulties by replacing S_{2dis} with a positive value. For large rotational numbers J_1, the half-widths calculated by the classical ATC model, which do not take account of the dispersion contribution ($S_{2dis} = 0$, curves 1), are at variance with experiment (Fig. 3). Two reasons are usually given for this[5]:

1) neglect of the short-range part of the potential, or

2) errors In the gas-kinetic cross section calculations.

In fact, as our calculations using our refined version of the ATCF model show (Fig. 3, solid curve), it appears quite sufficient to merely update the values of $\bar{b}(i)$ and $\bar{v}_2(i)$ using the dependence of the relative velocity upon the internal state of the absorbing molecule. In contrast with the conventional ATC model, taking account of the dispersion contribution S_{2dis} (solid curve) provides a good fit to the experimental data for both small and large J_1. Note that for CO_2—CO_2 our curve agrees fairly well with the data obtained by the BR model (Fig. 3, dotted line).

It should be pointed out that for the γ and δ calculations, the averaging over collisions $\left(\sum_{J_2}\rho_{J_2}\right)$ was carried out for $J_2 = 0$ up to $J_2 = 2 \cdot J_{max}$, where J_{2max} is the quantum number characterizing the most heavily populated rotational state of the buffer molecule.

The pressure-broadened half-widths CO_2—N_2 and CO_2—O_2 calculated by our model (Eq. (27)) for the ν_3 band are presented in Fig. 4 (solid lines). Also given for comparison are the results (dashed lines) from Ref. 5 obtained according to BR-theory.[4] As shown in Fig. 4, our results (solid line) provide a better fit to the experimental data than the results of Ref. 5. It should be emphasized that attempts to match the model (BR) to the experimental results led the authors of Refs. 4 and 5 to obvious contradictions. Thus, for example, for some reason or other, Robert and Bonamy and Rosenmann et al.[5] take different values of the quadrupole moment q (which is constant value) of the molecule of the buffer gas N_2 to describe absorption line broadening in various gases: $q_{N_2} = -1.5$ DÅ for CO—N_2 and $q_{N_2} = -1.3$ DÅ for CO_2—N_2. Tables IV and V compare some of the experimental half-widths reported by various authors with the values obtained by the proposed model.

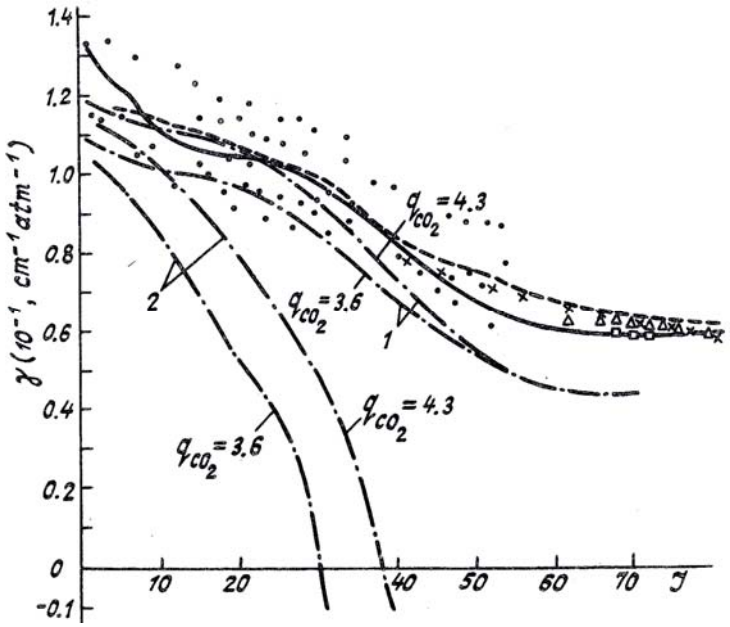

FIG. 3. Line half-widths of the vibrational ν_3 *band for* CO_2–CO_2 *at* $T = 300°K$. *Calculated: ATC model, curve 1 —* $\gamma(S_{2dis} = 0)$, *curve 2 —* $\gamma(S_{2dis} \neq 0)$, —— *our calculation;* ----- *BR-model.*[5] *Experimental:* Δ *— Ref. 12,* □ *— Ref. 13,* × *— Ref. 14,* • *— other authors.*

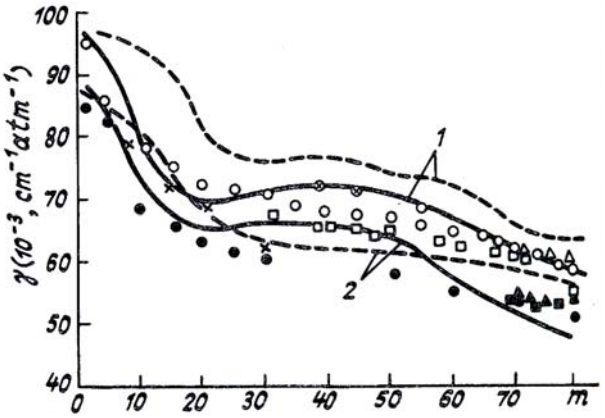

FIG. 4. Rovibrational half-linewidths of the ν_3 *band of* CO_2. *Curves 1 —* CO_2–N_2, *curves 2 —* CO_2–O_2. *Calculated: solid (27), (dashed) Ref. 5. Experimental for* CO_2–N_2: □– *Ref. 13,* Δ *— Ref. 12,* ⊗ *— Ref. 18,* ⊙ *— Ref. 14;* CO_2–O_2: ∎ *— Ref. 13,* ▲ *— Ref. 12,* ○ *— Ref. 14.*

TABLE IV. Self-broadened half-widths in the band centered at 961 cm^{-1} *(*$cm^{-1} \cdot atm^{-1}$*).*

P(16)	P(18)	P(20)	P(22)	P(24)	Reference
		0.096 (5)			18
0.106 (5)	0.105 (5)	0.096 (5)	0.100 (5)	0.094 (5)	19
0.109 (5)	0.107 (4)	0.105 (5)	0.106 (4)	0.104 (5)	20
			0.097 (10)	0.100 (10)	21
		0.0992 (20)			22
		0.102 (5)			23
0.100 (5)	0.098 (5)	0.096 (5)	0.094 (5)	0.092 (2)	24
0.107	0.106	0.105	0.104	0.103	this work

TABLE V. γ_{CO_2} *R-branch of* ν_3 *band* ($10^{-3}cm^{-1} \cdot atm^{-1}$).

	66	68	70	72	74	76	78	Reference
CO_2	59.5(6)	59.2(9)	59.4(4)			60.5	60.0	13
$-CO_2$			62.4		61.3	59.4	58.6	25
	64.5	64.0	63.5	62.5	61.5	60.5	59.5	12
	59.6	59.5	59.5	59.5	59.5	59.5	59.5	this work
CO_2	59.4(7)	59.9(7)	59.7(6)				55.2(15)	13
	61	61	60.5	60.5	60.0	60.0	60.0	12
$-N_2$	58	57					54	26
	64.1	63.4	62.5	61.4	60.2	59.2	58.4	this work
CO_2	55	53.4	53.2	54.8	54	54.7	56.3	13
$-O_2$	55	55	55	55	55	55	55	12
	54	52.5	51.2	50.0	49.0	47.6		this work

The experimental and calculated data are seen to agree well over a wide frequency range.

2.2. CALCULATED RESULTS FOR δ

In practice, in determining the line center shift taking into account the higher-order interactions (up to fourth-order) it is difficult to calculate δ in terms of the parameters $\bar{b}(i)$ and $\bar{b}(f)$. The orders can be readily accounted for by considering the average value of $\bar{b}(i, f)$ for the mixed state (Eq. (28)). In this case, however, there appears a systematic error, which can be estimated by comparing $\delta(\bar{b}(i), \bar{b}(f))$ and $\delta(\bar{b}(i, f))$ for the first- and second-order interactions only (Eq. (26)). The legitimacy of such an operation is related to .the fact that in the elements of the integrand expression (12) $(\tilde{S}_1 + \tilde{S}_2)(1 - S_2) = (\tilde{S}_1 + \tilde{S}_2) - (\tilde{S}_1 S_2 + \tilde{S}_2 S_2)$ for the shift it is clear that the first part $(\tilde{S}_1 + \tilde{S}_2)$ determines the line shift as given by Eq. (26) and the second part $(\tilde{S}_1 S_2 + \tilde{S}_2 S_2)$ for a fixed-type interaction consists of twelve elements:

$$\tilde{S}_{11} S_{21},\ \tilde{S}_{11} S_{2f},\ \tilde{S}_{11} S_{2m};$$

$$\tilde{S}_{1f} S_{21},\ \tilde{S}_{1f} S_{2f},\ \tilde{S}_{1f} S_{2m};$$

$$\tilde{S}_{21} S_{21},\ \tilde{S}_{21} S_{2f},\ \tilde{S}_{21} S_{2m};$$

$$\tilde{S}_{2f} S_{21},\ \tilde{S}_{2f} S_{2f},\ \tilde{S}_{2f} S_{2m}.$$

Eight elements from the set, similar to the elements S_{2m} from the real part S_2, depend on the mixed parameters $\bar{b}(i, f)$, and the remaining four elements $\tilde{S}_{11} S_{21}$, $\tilde{S}_{21} S_{21}$, $\tilde{S}_{1f} S_{2f}$, and $\tilde{S}_{2f} S_{2f}$ can be written as and $(\tilde{S}_{11} + \tilde{S}_{21}) S_{21}(\bar{b}(i, f))$ and $(\tilde{S}_{if} + \tilde{S}_{2f}) S_{2f}(\bar{b}(i, f))$. Such an approach is feasible, because the substitution of $S_2(\bar{b}(i), \bar{b}(f))$ for $S_2(\bar{b}(i, f))$ in calculating the half-width introduces an error of not more than 1% in the estimation of γ. It turns out that the last four elements as well as the first eight are mixed and, therefore; depend on $\bar{b}(i, f)$. Thus, the second part $(\tilde{S}_1 S_2 + \tilde{S}_2 S_2)$ can be expressed in terms of the impact parameter $\bar{b}(i, f)$. Then in the line shift calculations by Eq. (28) the error introduced by replacing $\bar{b}(i)$, $\bar{b}(f)$, by $\bar{b}(i, f)$ in Eq. (28) will be determined by the first part of the contribution to the line shift with $\tilde{S}_1(\bar{b}(i), \bar{b}(f)) + \tilde{S}_2(\bar{b}(i), \bar{b}(f))$ replaced by $\tilde{S}_1(\bar{b}(i, f)) + \tilde{S}_2(\bar{b}(i, f))$ which corresponds to the correction $\Delta = \delta(\bar{b}(i), \bar{b}(f)) - \delta(\bar{b}(i, f))$ to the line shift values obtained by Eq. (26).

The results of the foregoing analysis are presented in Fig. 5 for the *R*-branch of the vibrational band ν_3 for self-broadening of CO_2–CO_2. The dependences $\delta(\bar{b}(i), \bar{b}(f))$ and $\delta(\bar{b}(i, f))$ are obtained from Eq. (26) written in terms of the imaginary parts of the differential cross sections of the collision. One can see from Fig. 5 (cf. curves 1 and 2) that these dependences behave differently in different ranges of J_1. For J_1 = 6–25 the difference between $\delta(\bar{b}(i), \bar{b}(f))$ and $\delta(\bar{b}(i, f))$ is small (2–6%), while for J_1 = 30–60 it

amounts to 15–25%. On the contrary for $J_1 > 60$ the difference decreases and eventually disappears, since for large J_1, $\bar{b}(i)$, and $\bar{b}(f)$ are close to each other. The maximum difference, as seen from Fig. 5, is observed for $J_1 < 6$. Only a slight change is characteristic of $\delta(\bar{b}(i, f))$ for this range of J_1, while the change in $\delta(\bar{b}(i), \bar{b}(f))$ (curve 1) is more pronounced. An anomalous behavior of the dependence accompanied by a marked peak is observed for $J_1 = 4$.

The results obtained make it possible to determine the correction Δ for the entire range of values of J_1 under consideration. We also applied the correction to the calculations of $\delta(\bar{b}(i, f))$ made taking into account the third- and fourth-order interactions. These results are also plotted in Fig. 5.Here curve 3 is for the uncorrected values and curve 4 illustrates the results of the correction. As one can see from Fig. 5, the account of the contribution from the higher-order interactions (cf. curves 4 and 1) results in lower values of δ which differ by up to 30% for $J_1 \approx 6$–38. For $J_1 > 38$ the difference decreases and is $\leq 10\%$. A comparison of curves 3 and 4 shows that for the medium range of values of J_1 ($J_1 = 6$–20), the line shifts can be calculated with adequate accuracy by Eq. (28) without any correction. For .small and large values of the corrected and uncorrected values of the line shift differ drastically.

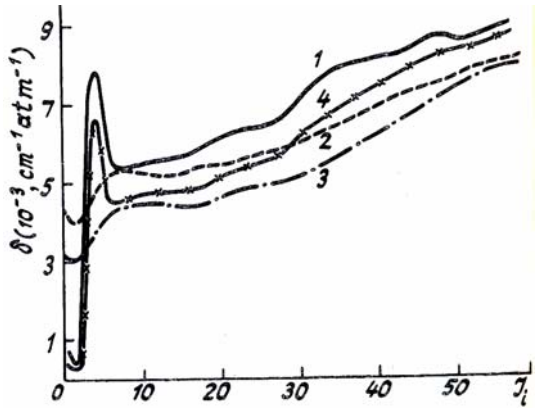

FIG. 5. CO_2–CO_2 *R-branches of* ν_3. *1) Eq. (26) with* $\bar{b}(i)$ and $\bar{b}(f)$, 2) Eq. (26) with $\bar{b}(i, f)$ 3) *Eq. (28) with* $\bar{b}(i, f)$ *and 4) Eq. (29) with* $\bar{b}(i, f)$.

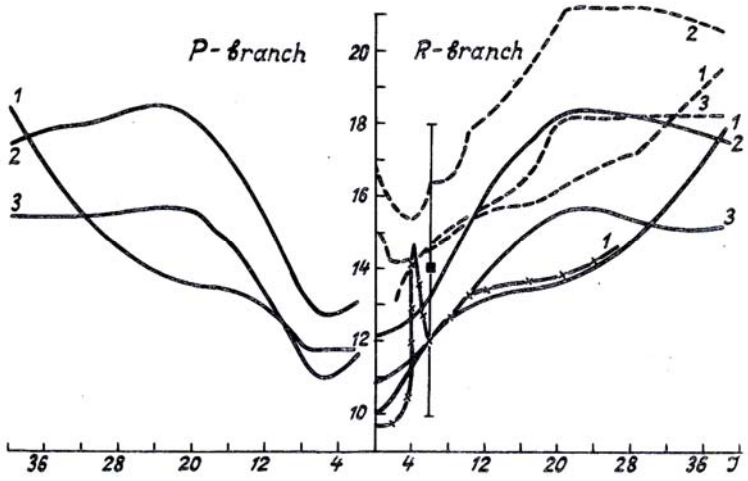

FIG. 6. Rovibrational line shifts in the $3\nu_3$ band at $T = 300$ K. *1)* CO_2–CO_2, *2)* CO_2–N_2, *3)* CO_2–O_2. ×-×- – *Eq. (28),* ----- *Eq. (26). Experimental:* ■ – CO_2–CO_2.[27]

Figure 6 gives the values of δ_{CO_2} in the absorption band $3\nu_3$ calculated for various collision partners. Our values for the *R*- and *P*-branches are plotted here. Also presented is the only experimental value $\delta_{CO_2-CO_2} = R(6) = -0.014$ cm^{-1} · atm^{-1} obtained in Ref. 26 with an error of ± 0.004 cm^{-1} · atm^{-1}, which agrees with ourcalculations (curve 1) within the measurement error.

A comparison of the calculations of δ for the CO_2 absorption bands ν_3 and $3\nu_3$ shows that the anomalous behavior of δ for small $J_1 = 0$…6 is smoothed out for the $3\nu_3$ band. We believe this is due to a greater degree of rotational excitation in the $3\nu_3$ band as compared to the ν_3 band ($\tilde{S}_{1dis}(3\nu_3) > \tilde{S}_{1dis}(\nu_3)$). One can expect that further growth of $\Delta\nu = \nu_f - \nu_i$, e. g., for the absorption bands $5\nu_3$ and $6\nu_3$, would lead to the disappearance of the anomalous peak.

Unfortunately, the lack of an appropriate set of experimental data on the spectral line center shifts prevents us from drawing the final conclusion as to the J_1-dependence of line shifts. Nevertheless, the results reported enable us to accentuate a number of critical points: 1) the use of the separate quantities $\bar{b}(i)$, $\bar{b}(f)$, $\bar{v}_2(i)$, and $\bar{v}_2(f)$ instead of $\bar{b}(i, f)$, and $\bar{v}_2(i, f)$ dramatically changes the shift values;

2) taking account of the contributions of the third- and fourth-order interactions yields, on the average, a 25–35% decrease in the shifts; and 3) the CO_2 absorption line shifts are sensitive to vibrational excitation.

It should be noted that the experimental data on the rovibrational line shifts in the $3\nu_3$ and 10.4 μm bands of CO_2–CO_2[27,28] makes it possible to determine how much the CO_2 polarizability changes in the molecular transition from the lower vibrational state (ν_{1n}, ν_{2n}, ν_{3n}, l_n) to the upper state (ν_{1b}, ν_{2b}, ν_{3b}, l_b). The dependence of the change in the polarizability in the transition from the lower vibrational state to the upper state, $\Delta\alpha$, via $K_{CO_2} = 0.17$ was found to be given by $\Delta\alpha = \Delta V \cdot K_{CO_2}$, where $\Delta V = \sum_{i=1}^{3} (|\nu_{1n} - \nu_{1b}|)$. The values of $\Delta\alpha$ obtained for the investigated bands are given in Table VI.

TABLE VI. Changes of the CO_2 polarizability in the investigated vibrational bands.

Band	ν_3	$3\nu_3$	10.4 μm
$\Delta\alpha$, Å^3	0.17	0.51	0.34

CONCLUSION

Our analysis of the calculated spectral llnewidths has shown that our model demonstrates as good an agreement between the calculated and the experimental values of γ as the BR-model,[4] but without requiring any additional fitting.

It should be emphasized that for $J_1 > 30$, especially for the CO_2–N_2 and CO_2–O_2 interactions, the values of $\bar{b}_{\min}(J_1)$ calculated by our model in the rectilinear trajectory approximation fall within the range $< 1.5 b_{gk}$, where the BR-model would predict curved trajectories. Since for the large rovibrational numbers J_1 our model is capable of reproducing the experimental data even better than the BR-theory, it can be assumed that for $b \lesssim 1.5 \cdot b_{gk}$, the particle trajectory will remain straight.

The refined ATCF model described here enables us to obtain both the absorption line half-widths and shifts using the same approximations and conditions. The line shifts calculated by our model agree with the experimental data within the measurement error. The BR-model, in contrast to our approach, was not checked for its feasibility to provide line center shifts.

Based on the proposed approach, a dialogue file system of calculated collisional parameters has been developed, which includes files of the temperature coefficients and the retaxational parameters (γ, δ).

Recently, γ and δ have been calculated for the absorbing molecules CO and NO. The results obtained also agree well with the experimental data. This will be the subject of a later paper. Work is underway to study the molecules HCl and H_2O, etc. In the future we will consider separately the problem of the temperature dependence of γ and δ. The dependence manifested in the internal state of the system is different for different temperatures.

REFERENCES

1. P.W. Anderson, Phys. Rev. **76**, 64 (1949).
2. C.J. Tsao and B. Curnutte, JQSRT **2**, 41 (1962).
3. Frost, J. Phys. B: Atom. Molec. Phys. **9**, No. 6, 1001 (1976).
4. D. Robert and J. Bonamy, J. de Physique **40**, No. 10, 923 (1979).
5. L. Rosenmann, J.M. Hartmann, M.Y. Perrin, and J. Taine, J. Chem. Phys **88(5)**, 2999 (1988).
6. J.S. Murphy and J.E. Boggs, J. Chem. Phys. **47**, No. 2, 961 (1967).
7. M.R. Cherkasov, Opt. Spektrosk. **42**, 45 (1977).
8. R.D. Sharma and W.R. Caledonia, J. Chem. Phys. **54**, 434 (1977).
9. *Reference Book of Physico-Chemical Values* (Khimiya, Leningrad, 1972).
10. R.P. Srivastava and H.R. Zaidi, Cam. J. Phys. **55**, 533 (1977).
11. G.A. Korn and T.M. Korn, *Mathematical Handbook for Scientists and Engineers* (Nauka, Moscow, 1973).
12. C. Cousin, R.Le Doucen, J.P. Houdean, C. Boulet, and A. Henry, Appl. Opt. **25**, 2434 (1986).
13. V. Malsthy Devi, B. Fridonich, G.D. Jones, and D.G.S. Snyder, J. Mol. Spectr. **105**, 61 (1984).
14 M. Margottin-Maclou, P. Dahoo, A. Henry, A. Valentin, and L. Henry, J. Mol. Spectr. **131**, 21 (1988).
15. Krishnaji and S.L. Srivastava, J. Chem. Phys. **41**, No. 8, 2266 (1964).
16. M.O. Bulanin, V.P. Bulychev, and E.B. Khodos, Opt. and Spektrosk. **48(5)**, 883 (1980).
17. D. Robert, M. Girand, and L. Galatry, J. Chem. Phys. **51**, 2192 (1969).
18. L. Losenraarm, M.Y. Perrin, and J. Taine, J. Chem. Phys. **88**, 2995 (1988).
19. S.R. Drayson and C. Young, JQSET **7**, 143 (1967).
20. J.T.K. McCubbin and T.R. Mooney, JQSRT **8**, 1255 (1966).
21. E. Arie, N. LaCome, and C. Rossetti, Can. J. Phys. **50**, 1800 (1972).
22. D. Dumitras, R. Alexandresen, and N. Comanicin, Rev. Rom. Phys. **21**, 301 (1976).
23. M.O. Bulanin, V.P. Bulychev, and E.B. Khodos, Opt. Spektrosk. **48**, 403 (1980).
24. R.S. Eng and A.W. Hants, J. Mol. Spectrosc. **74**, 331 (1979).
25. M.S. Abubakar and J.K. Shaw, Appl. Opt. **25**, 1996 (1986).
26. L.S. Rothman, Appl. Opt. **20**, 791 (1981).
27. P. Areas, E. Arle, and C. Boulet, J. Chem. Phys. **73(10)**, 5383 (1980).
28. Yu.G. Agalakov, M.O. Bulanin, V.V. Bertsev, A.P. Burtsov, and Yu.A. Rubinov, Opt. Spectr. **53**, No. 3, 493 (1985).